Devolatilization Characteristics and Kinetic Analysis of Lump Coal from China COREX3000 Under High Temperature

RUNSHENG XU, JIANLIANG ZHANG, GUANGWEI WANG, HAIBIN ZUO, ZHENGJIAN LIU, KEXIN JIAO, YANXIANG LIU, and KEJIANG LI

A devolatilization study of two lump coals used in China COREX3000 was carried out in a self-developed thermo-gravimetry at four temperature conditions [1173 K, 1273 K, 1373 K, and 1473 K (900 °C, 1000 °C, 1100 °C, and 1200 °C)] under N_2. This study reveals that the working temperature has a strong impact on the devolatilization rate of the lump coal: the reaction rate increases with the increasing temperature. However, the temperature has little influence on the maximum mass loss. The conversion rate curve shows that the reaction rate of HY lump coal is higher than KG lump coal. The lump coals were analyzed by XRD, FTIR, and optical microscopy to explore the correlation between devolatilization rate and properties of lump coal. The results show that the higher reaction rate of HY lump coal attributes to its more active maceral components, less aromaticity and orientation degree of the crystallite, and more oxygenated functional groups. The random nucleation and nuclei growth model (RNGM), volume model (VM), and unreacted shrinking core model (URCM) were employed to describe the reaction behavior of lump coal. It was concluded from kinetics analysis that RNGM model was the best model for describing the devolatilization of lump coals. The apparent activation energies of isothermal devolatilization of HY lump coal and KG lump coal are 42.35 and 45.83 kJ/mol, respectively. This study has implications for the characteristics and mechanism modeling of devolatilization of lump coal in COREX gasifier.

I. INTRODUCTION

THE COREX process is the first commercially operating smelting reduction process, which has been successfully applied in South Africa, South Korea, India, and China.[1,2] The biggest advantage of this process has realized the lump coal instead of coke to extract high quality hot metal, so the dependence on coking coal resources is reduced. The required quantities of lump coals are continuously charged into the gasifier at room temperature, as shown in Figure 1.[3,4] The gasifier is a dome-shaped countercurrent reactor, which can be divided into five zones from top to bottom: freebroad, fluidized bed, moving bed, raceway, and hearth.[4] The fast pyrolysis of lump coal is occurred at the freebroad under around 1373 K (1100 °C), which ensure the complete cracking of volatile matters released from coal. After the gasification reaction and mechanical extrusion at fluidized bed and moving bed, majority of the lump coal falls into the raceway to complete combustion reaction. A small number of lump coal stay in the hearth to form dead stock column and participate in the slag/iron–carbon reaction. The industry practice indicated that the properties of lump coal had a strong impact on the COREX performance.[5–8] The output of gas was determined by the pyrolysis properties of lump coal, and the permeability of burden was determined by the properties of lump char. Thus, it is important to understand the behaviors of lump coal at high temperature for improving the production efficiency of COREX process.

Degradation behavior of lump coal in COREX gasifier has been extensively investigated in the past. Kim[9] investigated devolatilization and cracking characteristics of five Australian coals. The study demonstrated that the cracking and swelling behaviors of coal were influenced by physical as well as chemical properties. Minkina[10] investigated devolatilization and the resulting char structure of six bituminous coals, from 20 to 40 mm in size, at 573 K to 1073 K (300 °C to 800 °C). The results noted that lump chars obtained from caking coal exhibited better resistance to breakage than their parent coals, while noncaking coals showed the opposite behavior. Sahoo[11,12] investigated degradation characteristics of weathered South Blackwater coal. It was found that the generation rate of coal fines increased with the increasing weathering period. Campbell[13]

RUNSHENG XU, YANXIANG LIU, and KEJIANG LI, Ph.D. Candidates, JIANLIANG ZHANG, Professor, and GUANGWEI WANG, ZHENGJIAN LIU, and KEXIN JIAO, Lecturers, are with the School of Metallurgical and Ecological Engineering, University of Science and Technology Beijing, Beijing 100083, China. Contact e-mail: zhang.jianliang@hotmail.com HAIBIN ZUO, Associate Professor, is with the State Key Laboratory of Advanced Metallurgy, University of Science and Technology Beijing.
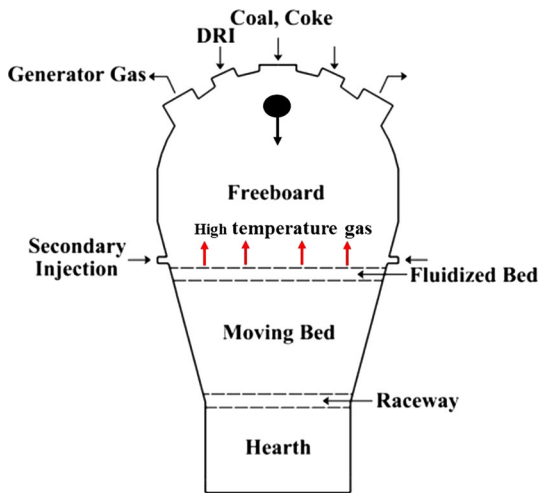
Fig. 1—Lump coal falling in the COREX melter gasifier.

investigated the agglomeration phenomenon of large coal particles (8 cm³ blocks) of three South African nonswelling coals. The results showed that the greater the tendency of lump coal to agglomerate, the greater the force needed to break the bond formed during devolatilization. Zhang[14] has investigated the structure characterization and metallurgical properties of the chars formed by devolatilization of lump coals. The study demonstrated that the characteristics of the produced chars were greatly affected by coal properties and carbonization conditions. Knepper[15] has investigated the pyrolysis, gasification, and combustion behaviors of different coals and coal briquettes. The results revealed that the biggest difference occurred during the gasification in CO_2, but the difference decreased with the increasing fuel particle.

Despite a series of researches on lump coals, there is limited information available about the pyrolysis kinetic mechanism of large coal particle especially used in COREX gasifiers. Kim[9] has studied the effect of coal size and temperature on the devolatilization reaction of lump coal by considering the first-order kinetics, but no further discussion on the mechanism model. Zhang[16] has investigated the high temperature pyrolysis behavior and kinetics of lump coal in COREX melter gasifier. It was found that three-dimensional diffusion was the primary restrictive link in the whole pyrolysis process of XLZ and DT lump coal. However, the research focused on the pyrolysis process of multi particles (about 50 g coals) and could not determine the most suitable mechanism function which described the whole reaction process.

In the present study, the reaction mechanism of fast pyrolysis of lump coal under high temperature was investigated. Various factors including maceral composition, crystalline structure, and functional groups were analyzed systematically. Three mathematical models including the random nucleation and nuclei growth model (RNGM),[17,18] volume model (VM),[19,20] and the unreacted core model (URCM)[21,22] were used to determine the kinetic parameters. It is expected that

this study will be useful in understanding of devolatilization process of lump coal and provide the information required for lump coal selection and operation in the gasifier.

II. EXPERIMENTAL

A. Preparation of Samples

Chinese COREX3000 has removed from Shanghai to Xinjiang, and it has already put into operation since June 2015, and the coals produced from Xinjiang area have fed into the gasifier as fuels. The standard requirements of lump coal are different for different COREX units. In order to ensure the regular operation and the efficiency of the production, more strict demand for lump coals used in COREX3000 was made to obtain better metallurgical performance. Therefore, the lump coals applied in Xinjiang COREX3000 were studied in this paper. Two lump coals were HY (produced in Hengyuan area) and KG (produced in Kuangou area).

In order to keep the identical physical dimensions and ensure the same experimental condition, the coal was shaped into coal cake ($20 \times 20 \times 20$ mm³) which was cut into a square piece from irregular lump coal, as shown in Figure 2. In order to remove the moisture (free water), the coal cake samples were vacuum dried for 10 hours at 313 K (40 °C).

B. Pyrolysis Tests

The schematic of self-developed thermo-gravimetry analysis device is shown in Figure 3.[23] This furnace is made up of electronic balance, heating furnace, gas control system, temperature control system, and data acquisition system. The range of the electronic balance is 1 kg, and the accuracy class is 0.001 g. The diameter of high quality pure alumina tube in the heating furnace is 60 mm. This furnace is heated with the $MoSi_2$ heating elements connected with a low-voltage and high-current power supply. The temperature of heating furnace can reach at 1773 K (1500 °C) at most. A thermocouple is located inside the working tube to monitor the temperature close to the sample. The reactor was operated under atmospheric pressure, and the heating rate was controlled by temperature setting software. The inert gas was introduced into the working tube to remove any residual oxygen, which flowed from the bottom of the heating furnace to top at a rate of 2 L/min. The experiment data were collected by data acquisition system through a computer. The data acquisition frequency was 6/s. When the temperature in the heating furnace reached to the setting value, the crucible with lump coal were carefully put into the furnace and hung on the hook at the bottom of the electronic balance, and the experiment data were begun to collect by computer at the same time. By the end of the experiment, the data were firstly saved, and then the crucible was quickly moved out to the N_2 container for cooling. The mass loss data of different coals were obtained through these pyrolysis tests.
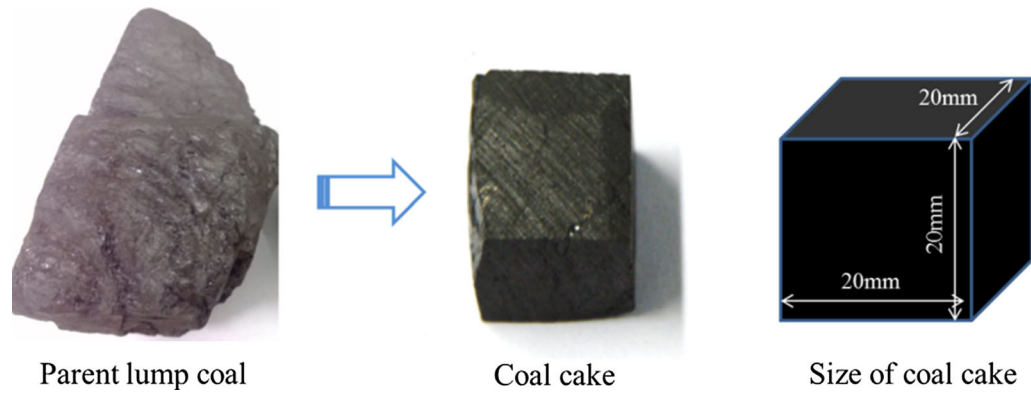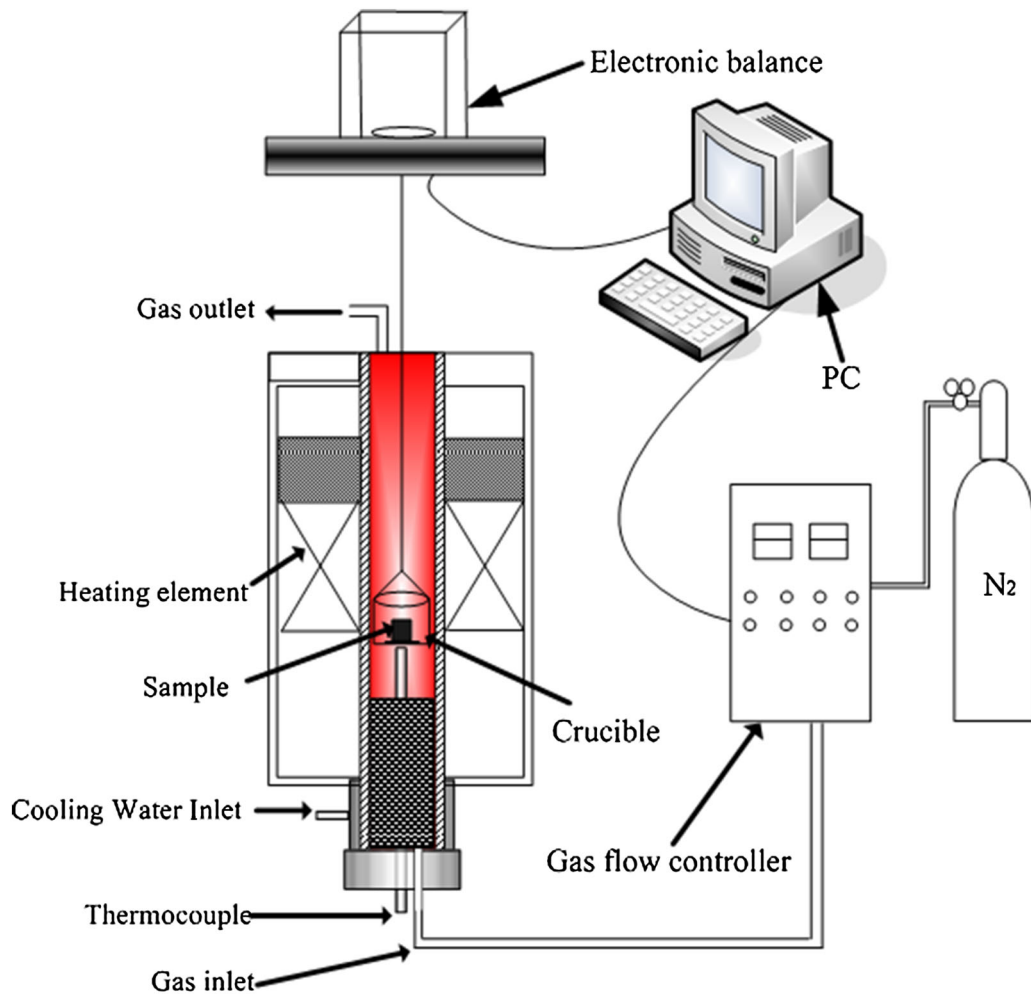
Fig. 2—The coal cake for pyrolysis.

Fig. 3—The schematic of experimental facilities for pyrolysis.

C. X-ray Diffraction

The carbon structure of lump coals was measured using a TTRIII multipurpose X-ray diffractometer made by Japan. All coals were crushed to fine powder of less than 0.074 mm in size before packing them into a holder. Copper Kα radiation (30 kV, 30 mA) was used as the X-ray source. The XRD spectra were obtained by scanning over an angular range (2θ) of 10 to 90 deg in a step of 2 deg/min.

D. FTIR Spectroscopy Analysis

The functional groups of lump coals were measured by NEX-US 470 FTRI spectrometer using the KBr pellet technique.[24] The FTIR spectra of the coals were

recorded over the range of 400 to 4000 cm^{-1}, and the total numbers of scan were 50 with spectral resolution of 4 cm^{-1}.

E. *The Properties Analysis of Lump Coal*

The properties of the lump coal samples are listed in Tables I through III. In order to get the content of coal ash, volatile, and moisture in air dry basis, proximate analysis was conducted according to the Chinese national standard GB/T212-2008. In order to get the contents of C, H, O, and S in coal, ultimate analysis was conducted according to the Chinese national standard GB/T214-2007, GB/T476-2008. The maceral analysis of lump coals was conducted by a DAS microscope (Leica DMRP RXP), which could magnify samples to 500 diameters. The maceral analysis method was based on the Chinese national standard GB 8899-88. The maximum vitrinite reflectance of lump coal was detected in accordance with the Chinese national standard GB/T 15591-1995. The chemical composition of coal ash was detected by X-ray fluorescence (XRF) using a Shimadzu sequential X-ray fluorescence spectrometer.

III. KINETIC MODELS

The devolatilization of coal has been studied by many researchers in the past few years.[25–27] Devolatilization is a complex physical and chemical reaction during coal pyrolysis process. The process of gas evolution and coal carbonizing may occur simultaneously during rapid pyrolysis at a high temperature for the lump coal used in COREX gasifier, which can be regarded as solid decomposition reaction. Devolatilization process of lump coal is more complex due to the influence of mass and heat transfer; thus, the macro-kinetic model is established in the present work. The devolatilization mechanism for lump coal is described as follows:

$$\text{Lump Coal} \rightarrow \text{Volatiles} + \text{Char}.$$

The reaction conversion rate of lump coal during isothermal devolatilization is the function of time and temperature, and it can be expressed as

$$\frac{d\alpha}{dt} = k(T)f(\alpha), \qquad [1]$$

where $\frac{d\alpha}{dt}$ is reaction conversion rate, s^{-1}; $k(T)$ is the reaction rate constant, which is the function of temperature; $f(\alpha)$ is the devolatilization mechanism function in differential form; t is devolatilization time, s; and α is devolatilization conversion.

$k(T)$ is calculated by Arrhenius equation:

$$k = A \exp\left(-\frac{E}{RT}\right), \qquad [2]$$

where A is the pre-exponential factor, s^{-1}; E is the activation energy, kJ/mol; and R is the universal gas constant, kJ/(mol K).

The devolatilization conversion is calculated by the following formula:

$$\alpha = \frac{m_i - m_t}{m_i - m_\infty}, \qquad [3]$$

where m_i is the initial weight of lump coal, g; m_t is the instant weight of the sample during experiment, g; and m_∞ is the sample weight after experiment, g.

The following formula can be obtained by Eqs. [1] and [2]:

$$\frac{d\alpha}{dt} = A \exp\left(-\frac{E}{RT}\right)f(\alpha). \qquad [4]$$

Table I. Proximate Analysis and Ultimate Analysis of the Coal Sample

	Proximate Analysis/Mass Percent, Air Dry Basis				Ultimate Analysis/Mass Percent, Dry Basis				
Sample	Moisture	Ash	Volatile	Fixed Carbon	C	H	N	St	O
HY	2.06	2.77	33.74	61.43	72.2	4.82	0.97	0.23	12.27
KG	1.89	2.64	23.26	72.21	77.28	3.86	1.00	0.25	9.61

Table II. Chemical Composition of Coal Ash (Mass Percent)

Sample	SiO$_2$	Al$_2$O$_3$	Fe$_2$O$_3$	CaO	MgO	TiO$_2$	SO$_3$	K$_2$O	Na$_2$O	MnO
HY	15.16	9.58	21.76	39.99	2.22	0.27	9.42	0.05	0.31	0.79
KG	13.67	5.70	27.42	32.23	4.46	0.49	13.68	0.08	0.95	0.36

Table III. Maceral Analysis of Coal (Percent)

Sample	Vitrinite	Exinite	Inertinite	Mineral	Reflectance of Vitrinite
HY	62.93	0.62	33.20	4.05	0.60
KG	48.30	0.00	43.65	8.85	0.71

Equation [4] is regarded as the relationships between devolatilization reaction rate and conversion. The curves of different mechanism functions can be obtained by nonlinear fitting. The corresponding activation energy and the pre-exponential factor can be calculated as well. If theoretical curves fit well with data curves obtained in the experiments, it indicates that the mechanism function which the theoretical curve stands for is the most optimum one.

In this paper, three mechanism functions were introduced to study the devolatilization kinetics, namely random nucleation and nuclei growth model (RNGM), volume model (VM), and shrinking unreacted core model (URCM).

The RNGM model[17,18] takes into account the random nucleation and nuclei growth during the reaction. When the devolatilization of lump coal is controlled by this model, the reaction mechanism functions can be expressed as follows:

$$\frac{d\alpha}{dt} = k_{RNGM}(1 - \alpha)\sqrt{-\ln(1 - \alpha)}. \qquad [5]$$

The VM model[19,20] assumes that the reaction uniformly distributes on both the outside and inside the particle surface. The reaction expression is given by

$$\frac{d\alpha}{dt} = k_{VM}(1 - \alpha). \qquad [6]$$

The URCM model[21,22] assumes that the reaction occurs gradually from particle surface to inside. With the reaction proceeding, the core of unreacted solid is shrinking. The reaction mechanism functions can be described as follows:

$$\frac{d\alpha}{dt} = k_{URCM}(1 - \alpha)^{2/3}. \qquad [7]$$

In the equations, k_{RNGM}, k_{VM}, and k_{URCM} are the reaction rate constant under different reaction mechanism functions.

Substituting Eq. [4] into Eqs. [5], [6], and [7], it can be obtained as follows:

$$\frac{d\alpha}{dt} = Ae^{-E/RT}(1 - \alpha)\sqrt{-\ln(1 - \alpha)}, \qquad [8]$$

$$\frac{d\alpha}{dt} = Ae^{-E/RT}(1 - \alpha), \qquad [9]$$

$$\frac{d\alpha}{dt} = Ae^{-E/RT}(1 - \alpha)^{2/3}. \qquad [10]$$

The values of E and A can be calculated from experimental data by employing nonlinear least-squares fitting methods. The objective function can be written as

$$OF = \sum_{i=1}^{N} \left(\left(\frac{d\alpha}{dt}\right)_{exp,i} - \left(\frac{d\alpha}{dt}\right)_{calc,i} \right)^2. \qquad [11]$$

The $\left(\frac{d\alpha}{dt}\right)_{exp,i}$ and $\left(\frac{d\alpha}{Et}\right)_{calc,i}$ represent the experimental data and estimated data, respectively, where i denotes the reaction temperature, K.

Equation [8] can be integrated to give

$$\alpha = 1 - \exp\left(-\left(-\frac{At}{2} \cdot \exp\left(\frac{-E}{RT}\right)\right)^2\right). \qquad [12]$$

Similarly, Eqs. [9] and [10] can be transformed into

$$\alpha = 1 - \exp\left(-At \cdot \exp\left(\frac{-E}{RT}\right)\right), \qquad [13]$$

$$\alpha = 1 - \left(1 - \frac{At}{3} \cdot \exp\left(\frac{-E}{RT}\right)\right)^3. \qquad [14]$$

The conversion curves can be obtained by introducing the previously calculated A and E into Eqs. [12] through [14]. In order to compare the experimental data and calculated values, the deviation (DEV) was calculated by the following equation:

$$DEV(\alpha)(pct) = 100 \times \frac{\left(\sum_{i=1}^{N}\left(\alpha_{exp,i} - \alpha_{calc,i}\right)^2 \big/ N\right)^{1/2}}{\max(\alpha)_{exp}}, \qquad [15]$$

where $DEV(\alpha)(pct)$ is relative error, pct; $\alpha_{exp,i}$ is experiment data; $\alpha_{calc,i}$ is calculated data; $\max(\alpha)_{exp}$ is the maximum conversion of experiment, and N is the number of experiment dada.

IV. RESULTS AND DISCUSSION

A. Thermogravimetric Analysis

1. *The comparison of devolatilization behaviors under different temperatures*

It can be seen from Figure 4 that the maximum mass loss of two lump coals increases a little with the temperature ranging from 1173 K to 1473 K (900 °C to 1200 °C). The differences of maximum mass loss of each lump coal under four temperatures are less than 1 pct. It indicates that the temperature has a little influence on the maximum mass loss in this experiment.

In addition, it is observed that the mass loss curves and conversion rate curves of two lump coals have a similar change rule, and all the conversion rate curves under different temperatures have one single peak. It indicates that the devolatilization processes of two lump coals under different temperatures are similar. Lump coal experienced very complex physical and chemical transformations while yielding volatile matter and generating coal char under high temperature. However, from the shape of conversion curves of two lump coals under high temperature, it can be deduced that the first degasification (cracking of bridges between the ring systems results in the formation of free radical groups,
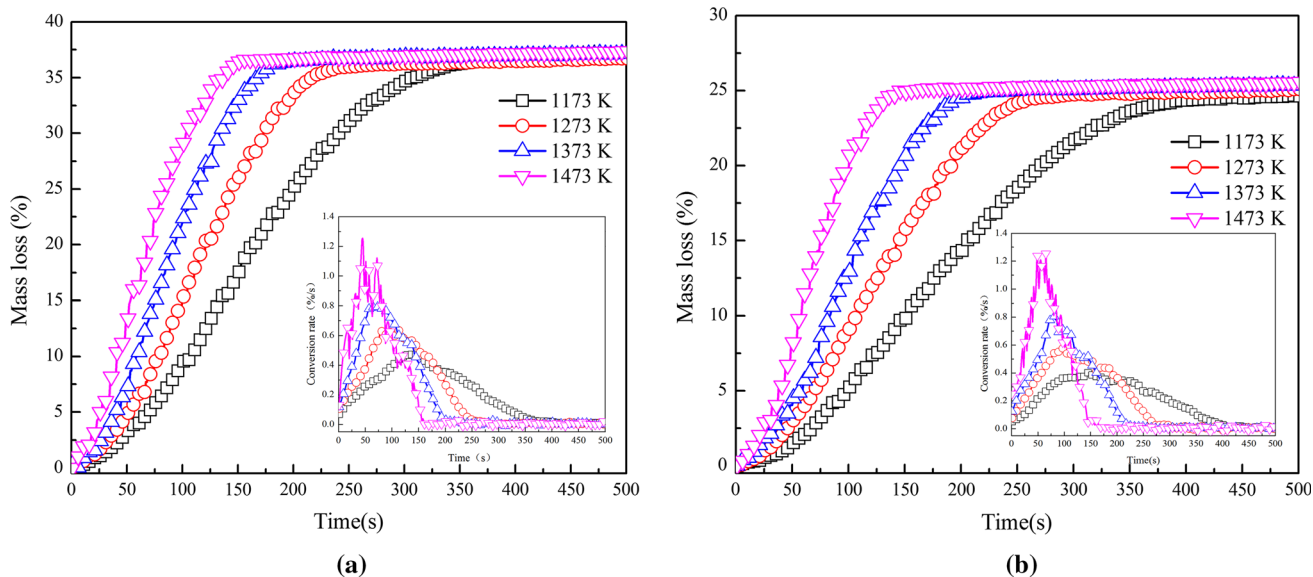
Fig. 4—The mass loss and conversion rate curves of lump coals: (*a*) HY coal, (*b*) KG coal.

Table IV. Devolatilization Characteristic Parameters of Different Lump Coals at Four Different Heating Temperatures

	Temperature [K(°C)]	Peak value of Conversion Rate (pct/s)	Reaction Time of Peak Value of Conversion Rate (s)	Final Conversion (pct)	Ending Time of Reaction (s)	$R_{0.5}$ (s^{-1})
HY	1173 (900)	0.49	146	37.66	410	0.0032
Lump coal	1273 (1000)	0.63	80	37.55	247	0.0043
	1373 (1100)	0.80	75	37.81	198	0.0056
	1473 (1200)	1.25	50	38.00	172	0.0075
KG	1173 (900)	0.41	147	25.18	422	0.0028
Lump coal	1273(1000)	0.57	94	25.55	273	0.0039
	1373 (1100)	0.79	83	25.82	221	0.0050
	1473 (1200)	1.25	51	25.95	174	0.0075

methane and gas, which is depolymerization reaction) and secondary degasification[28,29] (the coke/char and a small amount of gases are generated by the condensation of polynuclear aromatic compounds which is polycondensation reactions) proceed simultaneously without clear-cut distinction.

With the increasing temperature, the mass loss curve of lump coal gradually moves to the left, and the end time of devolatilization gradually reduces. This behavior indicates that with the increasing the working temperature, the devolatilization rate of lump coal increase. Meanwhile, the change rules of conversion rate curves of two lump coals with devolatilization temperature are also similar. With the increasing devolatilization temperature, the conversion rate curve peak becomes narrow and steep. It can be concluded that the devolatilization reaction gradually becomes severe with the increasing temperature. Furthermore, the devolatilization would complete in a shorter period. Devolatilization characteristic parameters of different lump coals are shown in Table IV. With the temperature ranging from 1173 K to 1473 K (900 °C to 1200 °C), the peak value of conversion rate of HY lump coal increases from 0.49 to 1.25 s^{-1}, and the end time of

devolatilization decreases from 410 to 172 seconds. The change trend of devolatilization parameters of KG lump coal with temperature is the same as that of HY lump coal. With the temperature ranging from 1173 K to 1473 K (900 °C to 1200 °C), the peak value of conversion rate of KG lump coal increases from 0.45 to 1.25 s^{-1}, and the end time of devolatilization reduces from 422 to 221 seconds. The results show that the temperature in COREX gasifier has a great influence on the devolatilization rate of lump coal. Based on the results mentioned above, it can be concluded that when the temperature of freeboard ranges from 1173 K to 1473 K (900 °C to 1200 °C) caused by fluctuation of COREX gasifier condition, the total output of gas can stay the same level, but the gas production rate will increase.

2. The comparison of devolatilization behaviors between different lump coals

Previous studies have indicated that the characteristics of coal have an important influence on its pyrolysis process.[29] The effects of coal rank on devolatilization of lump coal under high temperature were compared.

It can be observed from Figure 5, the conversion curve of HY lump coal is on the left side of the curve of KG lump coal at the working temperature ranging from 1173 K to 1373 K (900 °C to 1100 °C). However, the spacing of two curves reduces as the temperature increases from 1173 K to 1373 K (900 °C to 1100 °C), and the two curves overlap together at the working temperature 1473 K (1200 °C). The position change of two curves indicates that the rank of lump coal has great influence on the devolatilization behaviors below 1373 K (1100 °C), but this effect gradually reduces with the increasing temperature. It could be found that the effects of temperature on devolatilization process are more than coal properties during this experiment. With the working temperature at 1473 K (1200 °C), the devolatilization process of two lump coals is the same as observed in Figure 5(d). The characteristic parameters $R_{0.5}$[30] in Table IV can represent the conversion rate of lump coal under different conditions. With the increasing temperature, $R_{0.5}$ of HY lump coal changes from 0.0032 to 0.0075 s^{-1}, and that of KG lump coal changes from 0.0028 to 0.0075 s^{-1}. The reason for this phenomenon could be that the rank of two lump coals is at the same level, and severe depolymerization reaction and polycondensation reaction are occurred at the same time at 1473 K (1200 °C) in both two lump coals, and the difference of active components and heat transfer caused by the coal composition can hardly affect the pyrolysis reaction. The influences on the difference of devolatilization rate of two lump coals among 1173 K to 1373 K (900 °C to 1100 °C) were further discussed below.
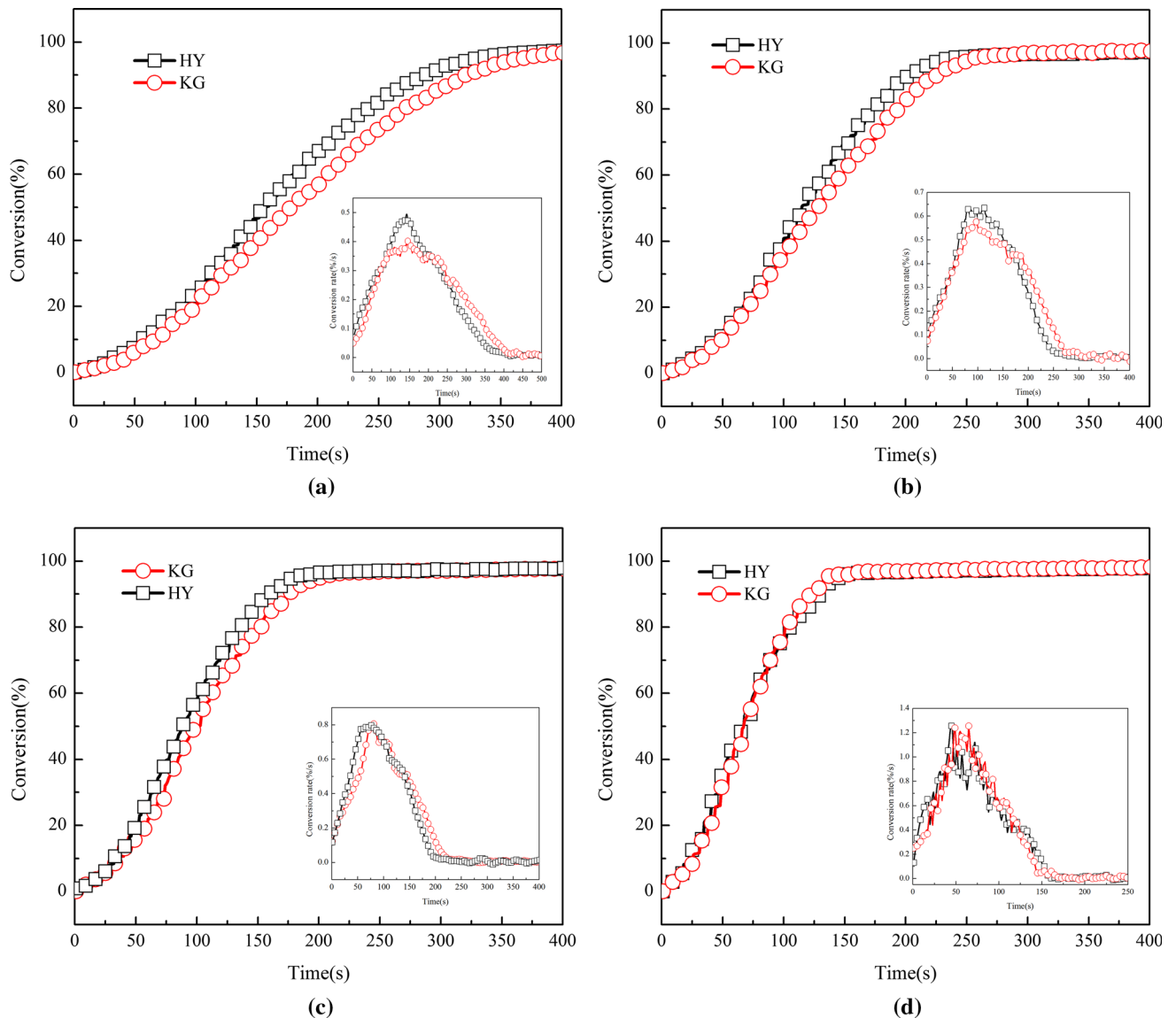

Fig. 5—The TG/DTG curves for lump coals under different temperatures: (a) 1173 K (900 °C), (b) 1273 K (1000 °C), (c) 1373 K (1100 °C), (d) 1473 K (1200 °C).

B. Correlation Between Devolatilization Rate and Properties of Lump Coal

1. The effects of composition on devolatilization rate

In order to explore the reason resulted in the difference of conversion rate of two lump coals at 1173 K to 1373 K (900 °C to 1100 °C), the chemical component, maceral composition, crystallite structure, and functional groups of two lump coals were investigated.

It can be found from Table I that the volatile content of HY lump coal is more than that of KG lump coal, but the ash content and moisture content are similar. From the perspective of the content of volatile matter, the metamorphic grade of KG lump coal is higher than that of HY lump coal. From the results of the ultimate analysis, the hydrogen content and oxygen content of HY lump coal are more than those of KG lump coal. Figure 6 shows the H/C ratio and O/C ratio of lump coals. It can be observed that H/C ratio and O/C ratio of HY lump coals are more than those of KG lump coal. Based on these results, it can be speculated that the contents of aliphatic side chain (like methyl (–CH$_3$), ethyl (–CH$_2$–CH$_3$), and propyl (–CH$_2$–CH$_2$–CH$_3$)) and oxygen functional group (like carboxyl (–COOH), carbonyl (=C=O), hydroxyl (–OH), methoxyl (–OCH$_3$), and ether bond (–O–)) of HY lump coal are more than those of KG lump coal.

The chemical composition of coal ash is shown in Table II. It can be found that the main compositions of coal ash are the oxides of calcium, iron, silicon, aluminum, magnesium, and sulfur, and the content of each oxides in two coal ashes are in the same level. From the point of view of ash composition and ash content, the differences of two coals are small, so the effects of ash on the devolatilization rate can be ignored. Therefore, the difference of devolatilization performance of two coals is mainly due to the differences of carbon matrix.

In addition, because both ash content and composition are extremely untypical, some information on the use of these coals in the COREX gasifier can be considered for operator. Low ash content in coal is welcomed for COREX operation, because low ash contributes to the reduction of slag quantity during COREX smelting. But the high CaO content in the coal ash should be considered, and the scheme of flux addition must be adjusted based on the CaO content to keep the final slag basicity steady.

2. The effects of coal maceral on devolatilization rate

Devolatilization reactions are complex, broadly involving bond breaking, vaporization, and condensation or cross-linking during the heating process, accompanying changes in the density of aliphatic group and aromaticity.[29] The ultimate product due to the condensation reaction is coke/char. From the research results of maceral analysis,[31–33] exinite has the highest hydrogen content and volatile matter, vitrinite contains the highest oxygen content, and inertinite has the highest carbon content. Figure 7 shows the coal maceral under the optical microscopy. The chemical stability and the structure of these macerals vary with their compositions. Vitrinite and exinite are considered active compositions, and inertinite is considered inert component. The weakest C–C bond in aliphatic bridge, as well as the C–C bond between alkyl and aromatic structures in exinite, is much easier to crack than other maceral structures, as shown in Figure 8.[34]

The content of active components (exinite, vitrinite) which can easily produce volatile in HY lump coal is much more than that of KG lump coal presented in Table III. Instead, the content of inactive components (inertinite) in HY lump coal is about 10 pct less than that of KG lump coal. This is the important reason which leads to the higher devolatilization rate of HY lump coal than KG lump coal from the maceral respect. So the devolatilization rate was promoted by the increase of active macerals (exinite and vitrinite). Based on the above-mentioned results, it can be concluded that the gas production rate in COREX gasifier can be improved by lump coal with high active maceral component contents.

3. The effects of microcrystalline structure on devolatilization rate

Carbon structures in coal determine the scattered X-ray intensities, as shown in Figure 9.[35] So, XRD is one of the important methods to investigate the microcrystalline structure of coal.[36] Often, the XRD curve of coal has four carbon peaks, indexed as (002), (100), (110), and γ. The (002) band at around 26 deg is generally considered the average stack height of the aromatic planes of carbon crystallite, while the (100) band at around 44 deg and the (110) band at around 81 deg are generally considered hexagonal structures. The γ band at around 16 to 23 deg is associated with the saturated structure such as aliphatic side chains or condensed saturated rings.[36–38]

The XRD spectra of two lump coals are shown in Figure 10. Two obvious peaks are observed: the (002) band and (100) band. The peak degrees are the same, but the shape of the peak of KG is steeper than that of HY, especially the (002) band. It indicates that the
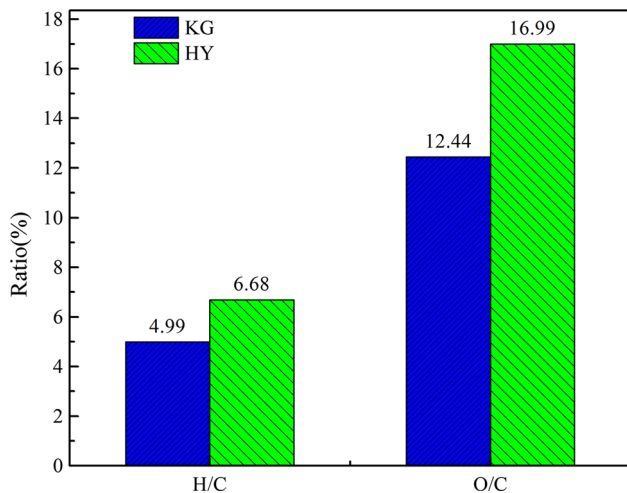
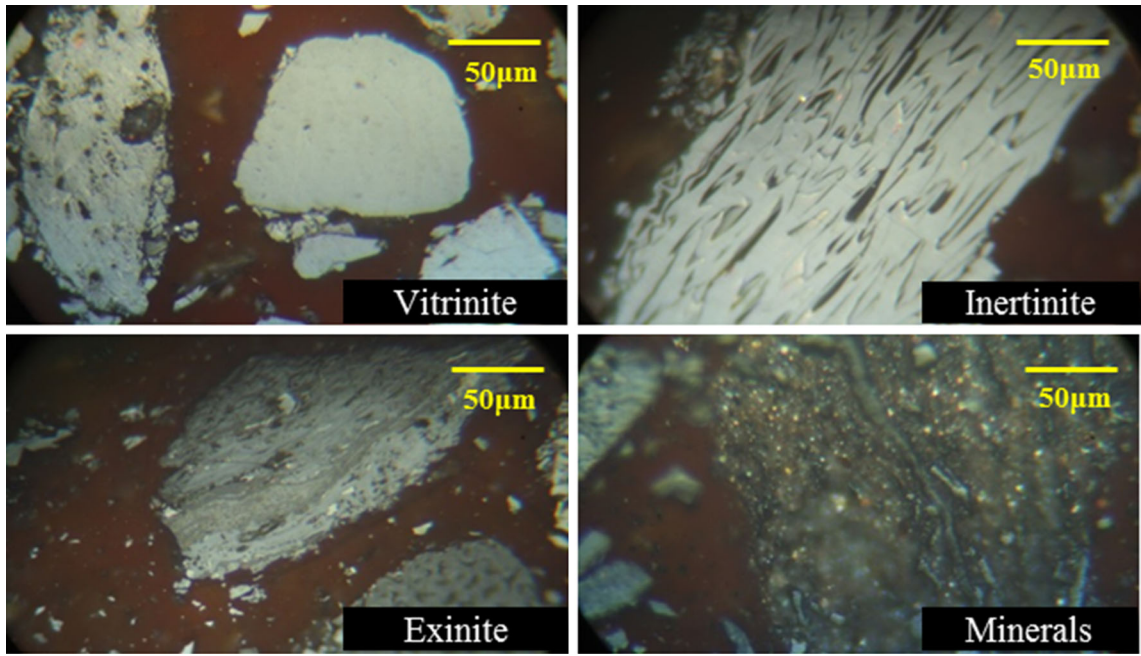Fig. 6— The H/C ratio and O/C ratio of lump coals.

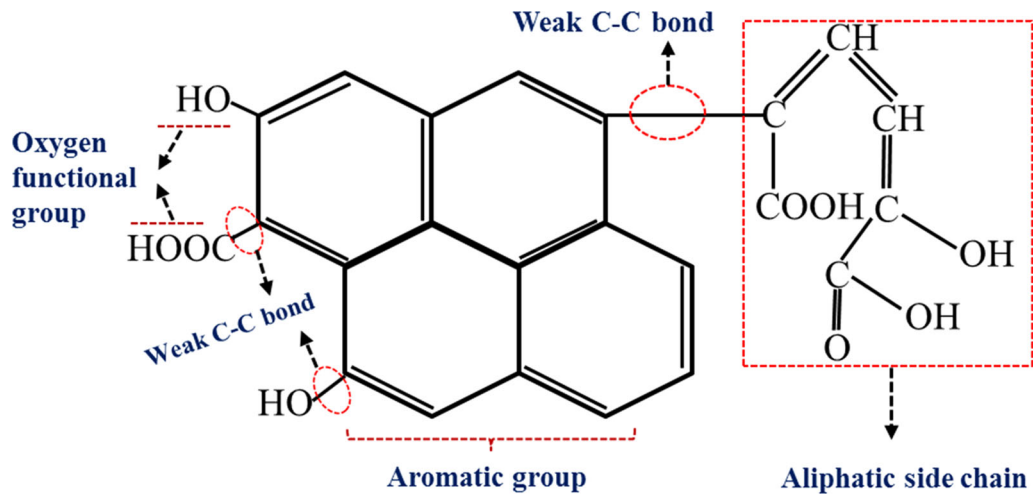Fig. 7—The coal maceral under the optical microscopy.

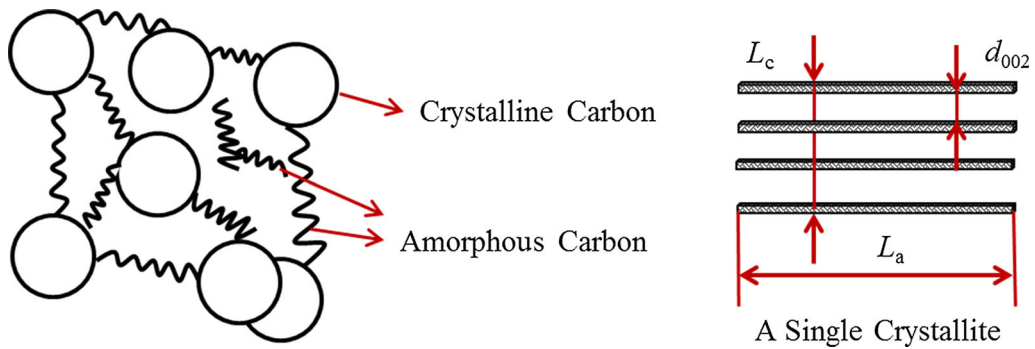Fig. 8—The schematic of the basic structure unit of coal.

Fig. 9—Schematic illustration of the simplified lump coal structure based on XRD observations.

degree of order of aromatic carbon layer in KG lump coal is more than that of HY lump coal, and the content of aliphatic side chains is less in KG lump coal. The structure parameters, such as interlayer spacing of the crystalline structure (d_{002}), crystallite sizes (L_a, L_c), layer number (n), and the aromaticity (f_a), can be calculated according to the Scherrer equation:[35]

$$L_c = \frac{0.89\lambda}{B_{002}\cos\phi_{002}}, \qquad [16]$$

$$L_a = \frac{K_1\lambda}{\beta_{100}\cos\theta_{100}}, \qquad [17]$$

$$d_{002} = \frac{\lambda}{2\sin\phi_{002}}, \qquad [18]$$

$$n = \frac{L_c}{d_{002}}, \qquad [19]$$

$$f_a = \frac{A_{002}}{A_{002} + A_\gamma}, \qquad [20]$$

where B_{002} is the half width of (002) band, deg; ϕ_{002} is the diffraction angle of (002) band, deg; λ is the wavelength of incident rays, nm; θ_{100} is the diffraction angle of (100) band, deg; β_{100} is the half width of (100) band, deg; and K_1 is correction coefficient, 1.84. A_{002} is the area of (002) band, and A_γ is the area of γ band. The calculated results of crystalline structure parameters of lump coals are shown in Table V.

It can be found from Table V that the average stacking height (L_c) of the layer structures in KG lump coal is higher than that of HY lump coal. The average lateral sizes (L_a) of the layer structures and interlayer spacing (d_{002}) of the crystallite structure in these two lump coals are similar. So the layer number of the crystallite structure in KG lump coal is more than that of HY lump coal. It indicates that the orientation degree of the crystallite structure, as well as the condensation degree of aromatic in KG lump coal, is higher. Moreover, the aromatic degree of KG lump coal is higher than that of HY lump coal, which can deduct that HY lump coal has more aliphatic side chains. Some research indicated that C–C bonds at the bridge between the ring systems were much weaker than other C–C bonds.[29] The pyrolysis begun with the cracking of bridges between the ring systems resulted in the formation of free radical groups. Therefore, the devolatilization rate of HY lump coal is higher than KG lump coal owning to its less aromaticity and orientation degree of the crystallite structure. Based on these results, in order to improve the gas production rate of COREX gasifier, the lump coals with less aromaticity and orientation degree are more likely to be used.

4. The effects of functional groups on devolatilization rate

The coal is mainly composed of aromatic nucleus and surrounding the side chain, bridge bond, and functional groups. Most of functional groups are oxygen functional groups, and the remaining are small amounts of nitrogen/sulfur functional groups. Bridge bond is the chemical bonds to make the basic structure unit of coal link together as shown in Figure 8.

During the devolatilization process, the aliphatic side chain, bridge bond, and functional groups will crack, but the cracking energy varies with the groups. Some research found that the aliphatic side chain and bridge bond had better pyrolysis reactivity, followed by oxygen functional groups, and the thermal stability of the aromatic structure was best.[39]

The groups information of two lump coals were tested by FTIR, and the spectra are shown in Figure 11. It can be found that the –CH₃ stretching vibrations at 1380 and 2922 cm^{-1}, and the –CH₂/–CH₃ stretching vibrations at 1429 cm^{-1} in HY lump coal are more remarkable than those in KG lump coal. It indicates that the structure of aliphatic in HY lump coal is more than that
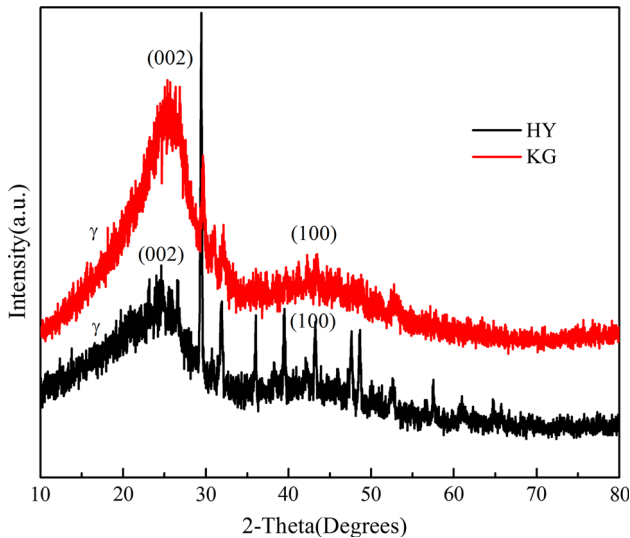

Fig. 10—The XRD spectrum of different lump coals.

Table V. Crystalline Structure Parameters of Lump Coals

Coal	$2\theta_\gamma$ (deg)	$2\phi_{002}$ (deg)	$2\theta_{100}$ (deg)	d_{002} (0.1 nm)	L_c (0.1 nm)	L_a (0.1 nm)	f_a	n
HY	16.58	25.38	42.22	3.51	7.68	8.73	0.52	2.19
KG	17.42	25.33	41.29	3.51	10.21	8.01	0.78	2.91

in KG lump coal. In addition, the –OH stretching vibrations at 3432 cm^{-1}, the =C=O stretching vibrations at 1599 cm^{-1}, and the –O– stretching vibrations at 1260 cm^{-1} in HY lump coal are also higher than those in KG lump coal. However, the absorption bonds at 678, 769, 813 cm^{-1} deriving from the aromatic ring in HY lump coal are less than those in KG lump coal. It can be concluded that HY lump coal has more oxygenated functional groups and less aromatic ring than KG lump coal, which results in the higher devolatilization rate of HY lump coal. Therefore, the lump coal with more oxygenated functional groups and less aromatic ring is appealed to use in COREX gasifier to improve the gas production rate.

Through this part research, the following experience for COREX operator can be reached: The devolatilization rate of lump coal is determined by gasifier temperature and the properties of coal, so the gas production

rate of gasifier can be controlled by the dome temperature adjustment and coal selection. However, when the dome temperature is above 1473 K (1200 °C), optimal selection of coal hardly affects the gas production rate. Furthermore, high dome temperature can lead to the temperature increase of export gas, and then more cold gas should be added to let the export gas cool to 1123 K (850 °C). This operation will result in more heat loss. Therefore, the method to increase the gas produce rate of COREX gasifier should be optimal selection of coal firstly. Namely, the coals which contain more active macerals (exinite and vitrinite), less aromaticity and orientation degree of the crystallite structure, and more oxygenated functional groups are the preferred for feeding into the COREX to improve the gas production rate.

C. Kinetic Parameters

The scatterplots in Figure 12 represent the relationship between conversion and conversion rate of the coal devolatilization under different temperatures. It can be observed that the conversion rate increases with the increasing working temperature. For a setting temperature, the conversion rate of devolatilization first increases with the conversion and then decreases after the conversion rate meets with its peak value. This phenomenon could be explained by the following reason: At the early stage of reaction, the cracking of functional groups in lump coal was gradually occurred with the increasing temperature of lump coal by absorbing the oven heat. So the reaction rate depended on the coal temperature before the peak value of the conversion rate. However, when the pyrolysis reaction approached to a certain extent after the coal temperature reached the working temperature, the surface area and activity site of lump coal were gradually reduced. When the inhibit effect caused by the reducing of surface area and activity site were greater than the promotion effect of temperature, the conversion rate met with its
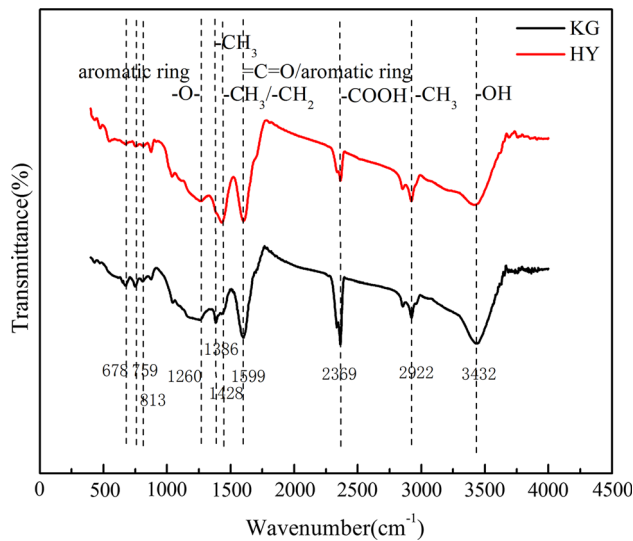

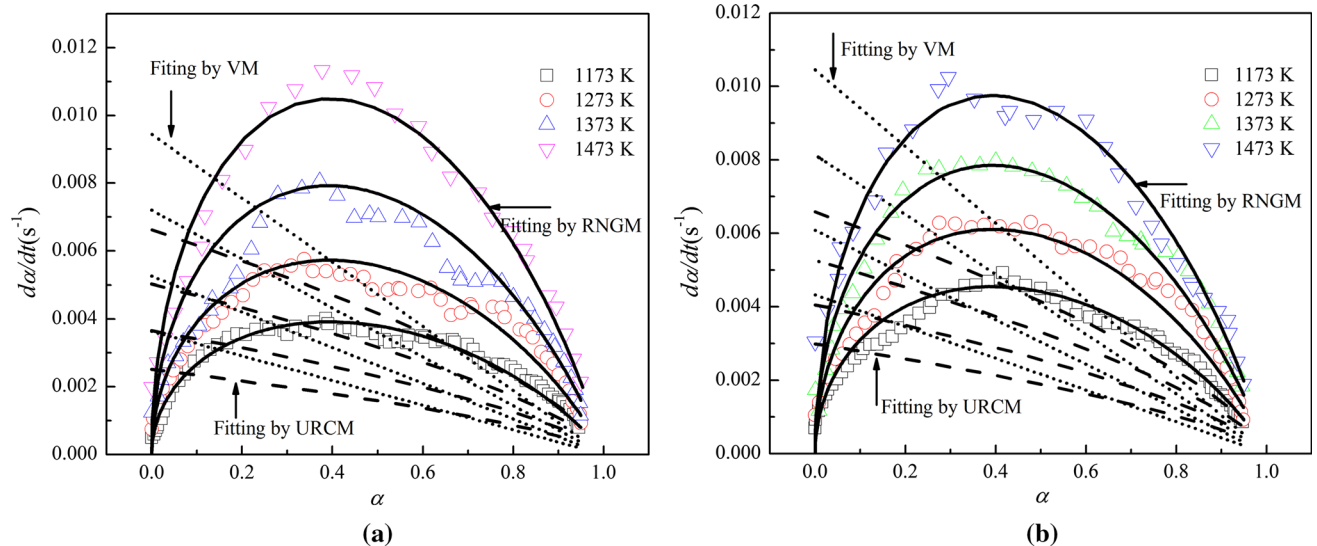Fig. 11—Infrared spectral resolution of different lump coals.

Fig. 12—Devolatilization rates of lump coals and fitting curves of RNGM, VM, and URCM: (a) KG coal, (b) HY coal.

peak value, and then the conversion rate decreased with the increase of conversion in the subsequent reaction time.

The devolatilization kinetics of lump coals were analyzed by the RNGM, VM, and URCM model explained in chapter III, respectively. The value of the kinetic parameters of lump coals under the heating temperatures of 1173 K, 1273 K, 1373 K, and 1473 K (900 °C, 1000 °C, 1100 °C, and 1200 °C) are presented in Table VI. The devolatilization conversion rate can be calculated based on Eqs. [8] through [10]. The lines in Figure 13 represent the calculation curves using the parameters obtained from the experiment data at different heating temperatures. On comparing the calculation curves and experimental curves, it can be found that the theoretical curves calculated by RNGM model almost overlap with the experimental curves.

In order to evaluate the simulating effect between the calculated value and experimental value in different models, the errors between calculation value and experimental value (DEV) are calculated by Eq. [15], and the results are presented in Table VII. It can be found that RNGM model has the highest accuracy in three models, and the deviation value is less than 1.87 pct, while the relative errors in VM model and URCM model are remarkably larger. It can be concluded that RNGM model is better than VM model and URCM model for the simulation of devolatilization process of lump coals.

All the results show that the devolatilization behaviors of lump coals satisfy the random nucleation and nuclei growth model. As the pyrolysis reaction proceeds at high temperatures, the liquid phase in the lump coal will form, and then the generated liquid phase transforms into solid state. During this process, the solid particles are capable of acting as the nuclei, and being wrapped by the liquid phase. Then the aggregation and growth of these small clusters will continue to occur. In contrast, the reaction rate has decreased along with the devolatilization reaction in the VM model and URCM

Table VI. Kinetic Parameters of the Lump Coals During Fast Devolatilization Under High Temperatures for Three Reaction Models

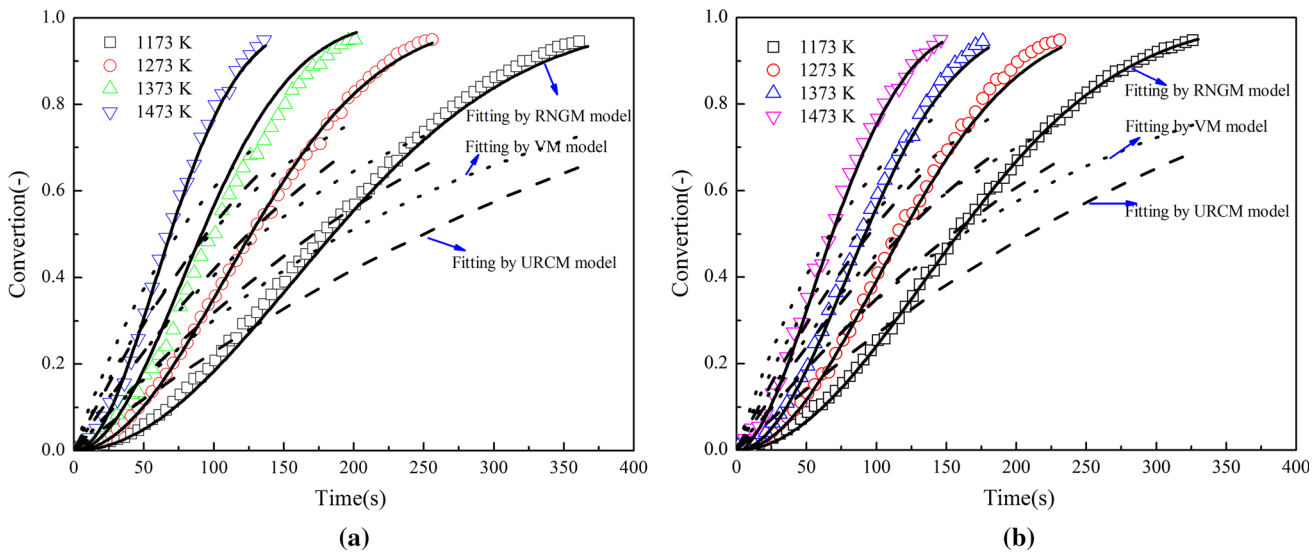| Sample	RNGM			VM			URCM		
	E (kJ/mol)	A (s^{-1})	R^2	E (kJ/mol)	A (s^{-1})	R^2	E (kJ/mol)	A (s^{-1})	R^2
HY	36.59	0.4468	0.9633	42.35	0.3284	0.4549	37.80	0.1427	0.3787
KG	47.40	1.1604	0.9585	45.83	0.3941	0.4787	46.46	0.2906	0.4082

Fig. 13—Relationships between experimental curves and calculated curves: (*a*) KG coal, (*b*) HY coal.

Table VII. Deviation Between the Experimental Data and Calculated Conversion Data

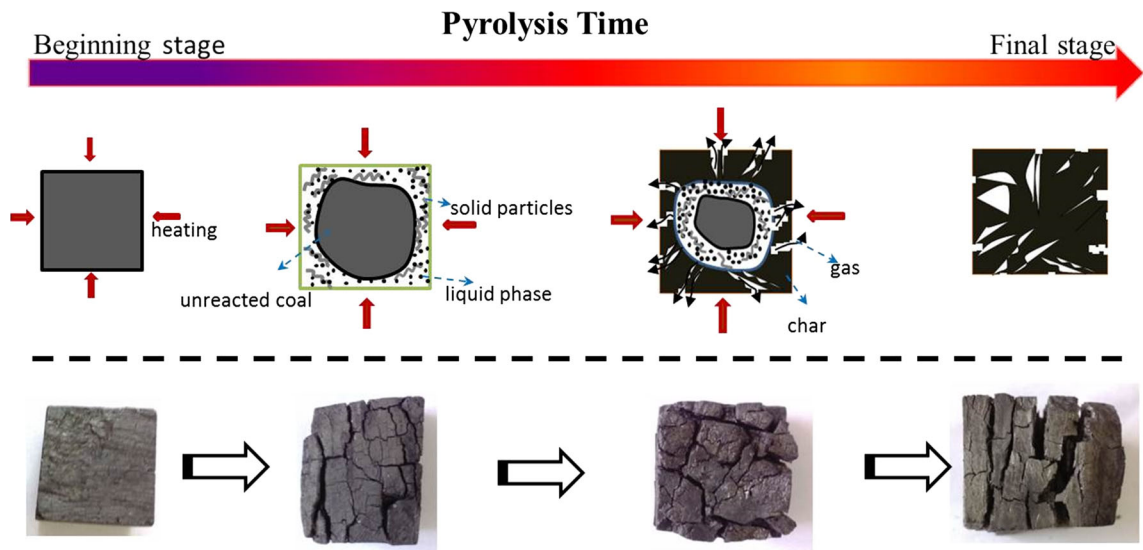| Sample	DEV(α) (pct)		
	RNGM	VM	URCM
HY	1.87	10.74	14.16
KG	1.21	10.54	15.46

Fig. 14—The pyrolysis process of lump coal under high temperature.

model, so they cannot well simulate the coal pyrolysis process. The schematic diagram of reaction mechanism of pyrolysis process is shown in Figure 14.

The devolatilization activation energies of HY lump coal and KG lump coal calculated by RNGM model are 42.35 and 45.83 kJ/mol, respectively, denoting the activity of devolatilization reaction of HY lump coal is better than that of KG lump coal. Therefore, the higher reaction rate of HY lump coal attributes to its lower reaction activation energy from the perspective of kinetic parameter analysis.

V. CONCLUSIONS

The characteristics and influence factors of the devolatilization process of lump coals used in COREX3000 under high temperature conditions were determined in a laboratory furnace. The reaction mechanism function of devolatilization process of lump coal was determined by master curve method followed by the calculation of the kinetic parameters. On the basis of this study, the following conclusions are drawn:

1. The pyrolysis tests demonstrated the strong influence of temperature on the devolatilization rate of lump coal, namely the devolatilization rate increased with the increasing temperature. However, the temperature had little influence on the maximum mass loss. The reaction rate of HY lump coal was higher than that of KG lump coal, which indicated that the reaction rate varied with the properties of coal. However, the difference of the reaction rate of two lump coals decreased with the increasing working temperature. It indicated that the temperature was the most important factor that determines the reaction rate in this study.
2. The difference of the devolatilization rate of two lump coals was found to depend on the properties of

carbon matrix. From the result of maceral analysis, HY lump coal contained higher active components (exinite and vitrinite), and less inactive components (inertinite). The spatial orientation degree and aromaticity of HY lump coal were smaller than those KG lump coal from crystal structure analysis. From the FTIR results, more oxygenated functional groups were detected in HY lump coal, precisely because above reasons leaded to the higher devolatilization rate of HY lump coal. Therefore, the coals which contain more active macerals (exinite and vitrinite), less aromaticity and orientation degree of the crystallite structure, and more oxygenated functional groups are preferred for feeding into the COREX to improve the gas production rate.
3. The results obtained by nonlinear fitting of mechanism functions showed that RNGM model was better than VM model and URCM model for the simulation of devolatilization process of lump coals, which indicated that the devolatilization process of lump coal satisfied the two dimension random nucleation and nuclei growth model. The devolatilization activation energy of HY lump coal and KG lump coal calculated by RNGM model are 42.35 and 45.83 kJ/mol, respectively.

NOMENCLATURE

XRD	X-ray diffraction
FTIR	Fourier transform infrared spectroscopy
RNGM	Random nucleation and nuclei growth model
VM	Volume model
URCM	Unreacted shrinking core model
$\frac{d\alpha}{dt}$	Reaction conversion rate (s^{-1})
$k(T)$	The reaction rate constant
$f(\alpha)$	The devolatilization mechanism function
t	Devolatilization time (s)
α	Devolatilization conversion
A	The pre-exponential factor (s^{-1})
E	The activation energy (kJ/mol)
R	The universal gas constant (kJ/(mol K))
m_i	The initial weight of lump coal (g)
m_t	The instant weight of the sample during experiment (g)
m_∞	The sample weight after experiment (g)
k_{RNGM}	The reaction rate constant of random nucleation and nuclei growth model
k_{VM}	The reaction rate constant of volume model
k_{URCM}	The reaction rate constant of unreacted shrinking core model
$\left(\frac{d\alpha}{dt}\right)_{exp,i}$	Reaction conversion rate based on the experiment data
$\left(\frac{d\alpha}{dt}\right)_{calc,i}$	Reaction conversion rate based on the experiment data
i	The reaction temperature (K)
$DEV(\alpha)$	Relative error (pct)
$\alpha_{exp,i}$	Experiment devolatilization conversion data
$\alpha_{calc,i}$	Calculated devolatilization conversion data
$max(\alpha)_{exp}$	The maximum conversion of experiment
N	The number of experiment dada
K_1	Correction coefficient
A_{002}	The area of (002) band
A_γ	The area of γ band

GREEK LETTERS

B_{002}	The half width of (002) band (deg)
ϕ_{002}	The diffraction angle of (002) band (deg)
λ	The wavelength of incident rays, nm
θ_{100}	The diffraction angle of (100) band (deg)
β_{100}	THE half width of (100) band (deg)

REFERENCES

1. S. Pal and A.K. Lahiri: *Metall. Mater. Trans. B*, 2003, vol. 34B, pp. 103–14.
2. S. Pal and A.K. Lahiri: *Metall. Mater. Trans. B*, 2003, vol. 34B, pp. 115–19.
3. X. Liu, G. Pan, G. Wang, and Z. Wen: *Energy Fuels*, 2011, vol. 25, pp. 5729–35.
4. K. Du, S. Wu, Z. Zhang, F. Chang, and X. Liu: *ISIJ Int.*, 2014, vol. 54, pp. 2737–45.
5. Y. Guo, W. Xu, J. Zhu, and J. Zhang: *Metall. Mater. Trans. B*, 2013, vol. 44B, pp. 1078–85.
6. P.P. Kumar, D. Gupta, T.K. Naha, and S.S. Gupta: *Ironmaking Steelmaking*, 2006, vol. 33, pp. 293–98.
7. Y.L. Guo, W. Xu, J. Zhu, and J. Zhang: *Ironmaking Steelmaking*, 2013, vol. 40, pp. 545–50.
8. P.P. Kumar, S.C. Barman, B.M. Reddy, and V.R. Sekhar: *Ironmaking Steelmaking*, 2009, vol. 36, pp. 87–90.
9. B. Kim, S. Gupta, S. Lee, and V. Sahajwalla: *Energy Fuels*, 2008, vol. 22, pp. 514–22.
10. M. Minkina, F.L.G. Oliveira, and V. Zymla: *Fuel Process. Technol.*, 2010, vol. 91, pp. 476–85.
11. R. Sahoo and D. Roach: *Powder Technol.*, 2005, vol. 152, pp. 1–8.
12. R. Sahoo and D. Roach: *Chem. Eng. Process.*, 2005, vol. 44, pp. 797–804.
13. Q.P. Campbell, J.R. Bunt, and F. de Waal: *J. Anal. Appl. Pyrol.*, 2010, vol. 89, pp. 271–77.
14. S. Zhang, H. Peng, X. Zhang, W. Liu, L. Wen, and G. Qiu: *Fuel Process. Technol.*, 2015, vol. 129, pp. 174–82.
15. M. Knepper, A. Babich, and D. Senk: *Proc. 6th Int. Congress on the Science and Technology of Ironmaking - ICSTI*, Rio de Janeiro, Brazil, 2012, pp. 811–21.
16. S. Zhang, F. Zhu, C. Bai, L. Wen, and H. Peng: *Ironmaking Steelmaking*, 2014, vol. 41, pp. 219–28.
17. L.T. Vlaev, I.G. Markovska, and L.A. Lyubchev: *Thermochim. Acta*, 2003, vol. 406, pp. 1–7.
18. L. Wang, J. Cai, M. Li, and H. Sun: *J. Northeast. Univ. (Nat Sci)*, 2010, vol. 31, pp. 550–54.
19. S. Kasaoka, Y. Sakata, and C. Tong: *Int. Chem. Eng.*, 1984, vol. 25, pp. 160–67.
20. J.Y. Shang and E.W. Eduard: *Fuel*, 1984, vol. 63, pp. 1604–09.
21. C. Xu, S. Hu, J. Xiang, H. Yang, L. Sun, S. Su, B. Wang, Q. Chen, and L. He: *Bioresour. Technol.*, 2014, vol. 171, pp. 253–59.
22. J. Szekely and J.W. Evans: *Chem. Eng. Sci.*, 1970, vol. 25, pp. 1091–107.
23. R. Xu, J. Zhang, G. Wang, H. Zuo, P. Li, H. Wang, H. Lin, and S. Liu: *J. Thermal Anal. Calorim.*, 2016, vol. 123, pp. 773–83.
24. H. Xiao, J. Zhang, F. Jia, and Q. Pang: *Iron and Steel*, 2014, vol. 49, pp. 29–33 (in Chinese).
25. B. Feng, S.K. Bhatia, and J.C. Barry: *Carbon*, 2002, vol. 40, pp. 481–96.
26. G. Wang, J. Zhang, X. Hou, J. Shao, and W. Geng: *Bioresource Technol.*, 2015, vol. 177, pp. 66–73.
27. Y. Sekine, K. Ishikawa, E. Kikuchi, M. Matsukata, and A. Akimoto: *Fuel*, 2006, vol. 85, pp. 122–26.
28. K. Xie: *Coal Structure and Its Reactivity, First Edition*, Science Press, Beijing, 2012, pp. 210–12.
29. J. Yu, J.A. Lucas, and T.F. Wall: *Prog. Energy Combust. Sci.*, 2007, vol. 33, pp. 135–70.
30. Y. Bai, Y. Wang, S. Zhu, L. Yan, F. Li, and K. Xie: *Fuel*, 2014, vol. 126, pp. 1–7.
31. L. Zhang, W. Liu, and D. Men: *Int. J. Min. Sci. Technol.*, 2014, vol. 24, pp. 93–98.
32. R. Walker and M. Mastalerz: *Int. J. Coal Geol.*, 2004, vol. 58, pp. 181–91.
33. W. Xie: *Coal Chemical and Coal Quality Analysis*, 1st ed., Metallurgical Industry Press, Beijing, 2012, pp. 22–25.
34. K. Xie: *Coal Structure and Its ReactivitM, First Edition*, Science Press, Beijing, 2012, pp. 68–70.
35. L. Lu, V. Sahajwalla, C. Kong, and D. Harris: *Carbon*, 2001, vol. 39, pp. 1821–33.
36. O.O. Sonibare, T. Haeger, and S.F. Foley: *Energy*, 2010, vol. 35, pp. 5347–53.
37. S. Gupta, V. Sahajwalla, P. Chaubal, and T. Youmans: *Metall. Mater. Trans. B*, 2005, vol. 36B, pp. 385–94.
38. M. Kawakami, H. Kanba, K. Sato, T. Takenaka, S. Gupta, R. Chandratilleke, and V. Sahajwalla: *ISIJ Int.*, 2006, vol. 46, pp. 1165–70.
39. P.R. Solomon, D.G. Hamblen, R.M. Carangelo, M.A. Serio, and G.V. Deshpande: *Energy Fuels*, 1988, vol. 2, pp. 405–22.